Technology and Health Care 15 (2007) 385–398
IOS Press

A method for a mechanical characterisation of human gluteal tissue

C. Then[a,b], J. Menger[a,b], G. Benderoth[a,b], M. Alizadeh[d], T.J. Vogl[a,c], F. Hübner[a,c] and G. Silber[a,b,*]
[a]*Center of Biomedical Engineering* (*CBME*), *Frankfurt/Main, Germany*
[b]*Institute for Materials Science, University of Applied Sciences, Frankfurt/Main, Germany*
[c]*Department of Diagnostic and Interventional Radiology, Hospital of the Johann Wolfgang Goethe University, Frankfurt/Main, Germany*
[d]*University of Science & Technology, Teheran, Iran*

Received 14 May 2007
Revised /Accepted 4 July 2007

Abstract. The most common complication associated with immobilization is pressure sores caused by sustained localized tissue strain and stress. Computational simulations have provided insight into tissue stress-strain distribution, subject to loading conditions. In the simulation process, adequate soft tissue material parameters are indispensable. An *in vivo* procedure to characterise material parameters of human gluteal skin/fat and muscle tissue has been developed. It employs a magnetic resonance imaging (MRI) device together with an MRI compatible loading device. Using the derived data as constraints in an iterative optimization process the inverse finite element (FE) method was applied. FE-models were built and the material constants describing skin/fat and muscle tissue were parameterized and optimized. Separate parameter sets for human gluteal skin/fat and muscle were established. The long-term shear modulus for human gluteal skin/fat was $G_{\infty,S/F} = 1182$ Pa and for muscle $G_{\infty,M} = 1025$ Pa. The Ogden form for slightly compressible materials was chosen to define passive human gluteal soft tissue material behaviour. To verify the approach, the human skin/fat-muscle tissue compound was simulated using the derived material parameter sets and the simulation result was compared to empirical values. A correlation factor of $R^2 = 0.997$ was achieved.

Keywords: Human tissue, separation of fat and muscle, material parameters, bed sore

1. Introduction

Pressure sores are immensely costly ($4 billion for the UK annually [3]) and cause severe trauma for the patient. As the population ages the situation could worsen. Health care products require better design to effectively reduce or eliminate bed sores and improve life quality. Implementing such design requires characterizing the interaction of human soft tissue with its support in a computational model.

Although pressure sore development is multifactorial, it is commonly agreed that sustained mechanical tissue loading plays a significant role during sore formation. The magnitude of the tissue loading is just

*Address for correspondence: G. Silber, Institute for Materials Science, University of Applied Sciences, Nibelungenplatz 1, D-60318 Frankfurt am Main, Germany. Tel.: +49 69 1533 3035, +49 69 1533 3081; Fax: +49 69 1533 3030; E-mail: silber@fb2.fh-frankfurt.de.

as important as the duration of the applied load in estimating the risk of developing pressure sores [12]. It is believed that pathological stress and strain distribution leads to limitation of the nutritive blood flow to the microvasculature. Hypoxic injury to the affected cells and breakdown of the metabolic cell processes are the consequence [11,24]. Observational studies have shown that most pressure sore development is a progressive process originating from deep subdermal layers, spreading to superficial dermal and then epidermal layers [23]. This has been confirmed by Linder-Ganz and Gefen [15] who showed that deeper muscle tissue exhibits a higher sensitivity to pressure related injuries than more superficial tissues.

Employing computational simulation methods which take human anatomy and mechanical soft tissue properties into account, the stress-strain distribution subject to body-weight loading in a seated or recumbent position can be visualized and quantified in deeper tissue areas. Several empirical studies investigating the stress-strain state of human soft tissue have been carried out, relying on material parameters which have been derived with different methods. Specifically, buttock indentation tests have been performed by Todd and Thacker [32] and the soft tissue compound was assumed to be linearly elastic ($E = 15.2$ kPa, $\nu = 0.49$ for supine male). Based on animal studies, Oomens et al. [20] used rat data to represent human muscle tissue ($\mu_1 = 12$ kPa, $\alpha_1 = 30$) and skin parameters ($\mu_1 = 16$ kPa, $\alpha_1 = 10$) derived from pig experiments using the Ogden form for incompressible materials. Fat parameters were assumed ($\mu_1 = 20$ kPa, $\alpha_1 = 5$). In an additional study of Oomens et al. [19], again, animal data was employed as a basis for the investigation. Using a neo-Hookean material model, Sun et al. [29,30] made assumptions for the material properties of skin ($E = 0.85$ MPa), fat ($E = 0.01$ MPa) and muscle ($E = 0.126$ MPa) using a Poisson's ratio of $\nu = 0.485$. Literature based parameters were used in a recent study by Lim et al. [13] using the Mooney-Rivlin material model to describe human soft tissue behaviour. Linder-Ganz and Gefen [14] used a neo-Hookean material model employing material data of porcine gluteal muscles as well as skin/fat data from indentation testing and downsized the instantaneous material constants to obtain the long-term material response. Following a combined MRI-numerical approach, they used MRI tissue deformation data as a boundary constraint to solve the FE-model for the imaged conditions.

Experimental methods evaluating the elastic properties of human soft tissue in superficial dermal regions *in vivo* have been presented by Gefen et al. [7] and Aoki et al. [2]. Whereas the latter used suction cup or pipette aspiration devices to evaluate the elastic modulus, Gefen et al. developed a tissue stiffness measurement method to evaluate human tissue properties near the body surface, finding plantar soft tissue to be in the following range for the elastic modulus: $E = 27 - 162$ kPa.

Measurements to characterise deeper human soft tissue regions do not permit the classical experimental set-up e.g. tensile or shear testing. Therefore, several methods have been presented in the past to overcome the obstacle of not being able to measure *ex vivo*. While *ex vivo* measurements guarantee defined boundary conditions, one difficulty when applying *in vivo* loading is keeping track of the deformed boundaries of the tissue layers as well as the forces acting at the tissue layer surfaces. To overcome this difficulty, combined methods using image processing, measuring and numerical techniques have been proposed. A basic idea in the numerical process was to parameterize the material constants and iteratively solve for the imaged boundary conditions, with the objective of minimizing simulation vs. experimental deviation. The parameter set minimizing the objective function sufficiently characterizes the material behaviour subject to the considered test conditions. This approach termed inverse finite element method (iFEM) has been successfully applied by many researchers determining human tissue parameters. Vuskovic et al. [34] presented an *ex vivo* method applied to a pig kidney using iFEM. Applying an iterative optimization method based on an optimizations algorithm by Nelder and Mead, Schrodt et al. [26] evaluated tissue properties of the human heel proposing the following material parameters for the long-term tissue behaviour ($\mu_1 = 7.422$ kPa, $\alpha_1 = 27.81$, $\mathrm{D}_1 = 2.695$ MPa^{-1}, $\nu = 0.495$) based on the

Ogden form for slightly compressible materials. A numerical-experimental method has been presented by Oomens et al. [21]. It consisted of optically tracking displacement markers attached to a loaded specimen and iteratively simulating the procedure by parameterizing the material constants. The objective was to minimize the deviation of the numerically obtained nodal displacements from their corresponding tracked marker displacements. A possible appliance in mechanical characterization of biological materials was assumed. Similarly, a possible basic concept has been introduced and proposed for application to human tissue by Tada et al. [31]. They used a coupled iterative MRI-FE-method, deforming a layered rubber block and tracking the material deformation.

Besides numerical techniques, both image processing as well as indentation testing are commonly used and well-established approaches to evaluate geometrical displacement, as well as force-displacement of human soft tissue [7,14,28–30,32].

The studies reviewed above have comprehensively presented the use of computational simulations of the stress-strain state inside human soft tissue and the deployed material properties. Techniques and efforts to derive human soft tissue parameters have also been described. However, there is still a paucity of information on human material parameters characterizing human long-term gluteal fat and muscle tissue properties in deeper tissue regions, which account for large deformations. Although many studies rely on (short-term) animal tissue data, there is lacking verification of long-term tissue material parameters gained from *ex vivo* animal testing with *in vivo* long-term human tissue material data.

The approach presented in this investigation is based upon a combined method including MR-imaging data as well as the iFEM-technique and indentation testing. It demonstrates how long-term human gluteal tissue parameters of skin/fat (skin and fat were considered as combined) and muscle can be derived *in vivo*. To model human soft tissue behaviour and account for large tissue deformations, the constitutive equation for non-linear, hyperelastic, slightly compressible materials, proposed by Ogden, was used. The present approach was to apply a stepwise and cyclic loading and unloading of the gluteal tissue by indentation testing, thereby achieving distinct tissue relaxation with the aim of separating the elastic from the inelastic material properties. The mechanical behaviour of human skin/fat and muscle was observed separately to obtain separate force-displacement curves for the two tissue components, serving as constraints in the parameter optimization process. This approach allowed the evaluation of separate material parameters for human skin/fat and muscle. Eventually, the derived material parameters permitted a comparison of *in vivo* long-term human gluteal material constants with *ex vivo* long-term animal experimental data.

2. Methods

The experimental protocol was approved by the ethical committee of the Hospital of the Johann Wolfgang Goethe University of Frankfurt and informed, written consent was obtained from the volunteer participating in this investigation.

2.1. Force-displacement data of human fat-muscle compound

Biological tissue is nonlinear and anisotropic, exhibiting a combination of elastic and inelastic behaviour. Relying on the finding that pressure sores in deeper tissue regions develop over minutes to several hours and in contrast, tissue stress relaxes over seconds (20–60 s) to a nearly constant level, only the long-term tissue response was accounted for in this investigation [22,27]. This requires separating elastic from inelastic tissue properties. For this purpose, a testing procedure proposed by James and Green [10], successfully applied by Hartmann et al. [9] and Lion [16] for rubber-like materials and Schrodt et al. [25] for polymer soft foams was used.

(a)

(b)

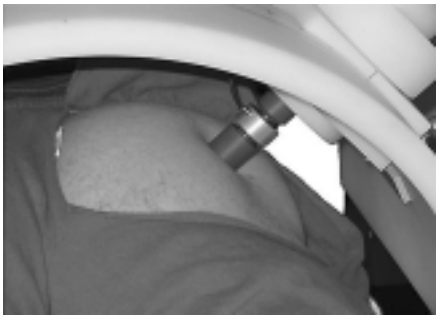

Fig. 1. (a) MR-compatible loading device, (b) Buttock loaded with a cylindrical indenter head.

2.1.1. Experimental set-up

To investigate the material behaviour of the skin-fat-muscle compound in the gluteus region, an MR-compatible loading device was developed (Fig. 1a) by which mechanical properties of the human body can be gathered *in vivo* (Fig. 1b). The apparatus ensures defined and reproducible loading and unloading and is compatible with the deployed MRI device in terms of material (PVC, AL) and dimensions (H $\times$ W $\times$ D 350 $\times$ 540 $\times$ 300 mm). The loading was applied via a cylindrical shaped indenter head (Ø25 mm) with a head corner radius of 1 mm equipped with a 200 N force transducer (1 mV/V$\pm$3%). The indenter displacement was measured via an incremental TTL-rotary encoder (1024 ppr) situated in the upper part of the apparatus. To localise the position of the indentation axis in the MRI-environment for reproducibility in the FE-modelling process, tablets with a high fraction of sodium hydrate were incorporated into the indenter head, conferring a clearly detectable signal. To ensure stability during measurement, the ground frame of the apparatus was fixed to the MRI table.

2.1.2. Location of the test point

The buttock was chosen as the indentation location since the pelvic bone offers a broadly based support which can be considered as very stiff compared to the buttock skin/fat and muscle tissue. The pelvic bone provides defined boundary conditions to guarantee reproducibility in the computational model. The gluteal region exhibited sufficient skin/fat and muscle tissue to provide a clearly distinguishable borderline between (deformed) fat and muscle tissue and bone structure in the MR-images. The test

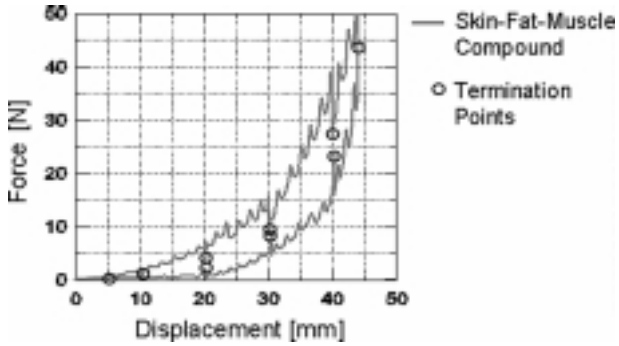

Fig. 2. Force-displacement data from a 35 year old male subject recorded at the gluteus.

person's hip region was fixed using a plaster mold fitting tightly into the base frame of the loading apparatus and embedding the pelvis such that it could not escape the outer loading. To minimize shear effects in the muscle-bone interface as well as in the fat-muscle interface, the indenter load direction was set almost orthogonal to the pelvic bone surface. This was verified by MRI prerecordings. The location of indentation relative to the pelvic bone was primarily chosen with respect to the pelvis bone acting as a counter bearing to completely carry the compressive indenter load. Thus, the indentation axis was centred to the bone surface, being aware that the gluteus medius muscle was partially compressed along with the gluteus maximus.

2.1.3. Indentation test

With the objective of separating the elastic from the inelastic tissue material properties, a stepwise and cyclic loading and unloading of the passive gluteal tissue with the subject in a procumbent, relaxed position was performed. A constant velocity (2 mm/s) was maintained with a total tissue indentation of 44 mm, while indenter force and indentation displacement were recorded, Fig. 2.

To eliminate frictional effects, the indenter was lubricated. After each deformation step, a holding time of two minutes was maintained where the indenter displacement was held constant and the tissue responded with a relaxation process. The force-displacement values reached after each holding period are referred to as termination points. The force values of the termination points almost reached a state of equilibrium. Corresponding termination points of the loading and unloading paths indicate the range comprising the pure elastic tissue behaviour and served as basic input for parameter identification. At maximum indenter displacement, tissue unloading was performed corresponding to the loading procedure.

The displacement increment sizes (0-5-5-10-10-10-4 mm) of the loading and unloading cycle were chosen to accommodate the total experimental time including seven MR sessions and test apparatus management. The first two increments intended to give higher resolution of the initial curve slope, providing minor force increase, whereas the magnitude of the last increment was due to limitation of the load impact on the test person. The maximum indenter displacement assured an intense ascent of the indentation force in order to capture a wide range of gluteal tissue behaviour.

2.2. MR-imaging and separation of in vivo human fat and muscle properties

2.2.1. MR-imaging

Transversal MR-images of the unloaded and stepwise loaded tissue in the gluteus region were performed as depicted in Fig. 3 for the initially undeformed configuration and the last deformation state at

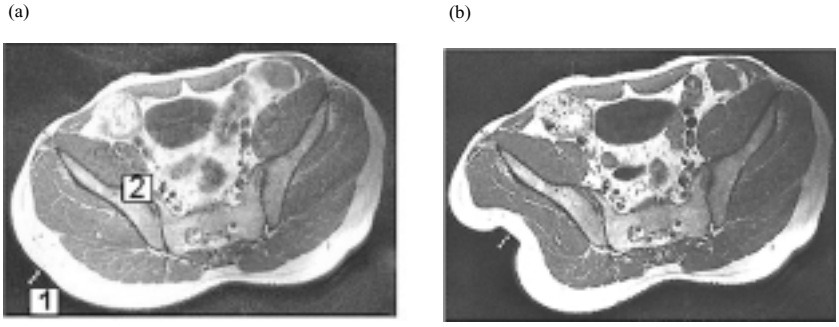

Fig. 3. Transversal MR-images of the buttock region showing tissue deformation at (a) 0.0 mm and (b) 44 mm indenter displacement.

$\Delta = 44$ mm. The tablets incorporated into the indenter head are displayed by the light spots 1 found at the lower left corner of Fig. 3a. With the aid of the pelvic bone 2, defined muscle tissue displacement and bearing of the indentation forces was achieved.

The data was acquired using a 1.5 T MAGNETOM SONATA® (Siemens, Erlangen/ Germany) scanner. The slice thickness was set to 2mm without a slice gap using a matrix size of 512×512. To initially detect the desired indenter position, a turbo spin echo sequence with transversal orientation and a repetition time (TR) of 3000 ms and an echo time (TE) of 93 ms was applied. For the actual scan of the gluteus, a turbo spin echo sequence was used with a TR of 5000 ms and a TE of 98 ms.

The process of MR-imaging and indentation testing were combined such that after each deformation step outside the MRI coil, the table was slid into the MRI where the buttock was scanned.

2.2.2. Separation of the mechanical properties of fat and muscle

In the gluteus region, the presented approach assumed a reduction of the complex tissue compound to a two-component model consisting of a skin/fat layer and a muscle layer. As the *in vivo* indentation experiment provided one force-displacement curve and termination points representing the tissue compound, the separation of skin/fat and muscle properties is based on the assumption of unique indenter force transmission through both tissue layers. Thus, combining the indentation force with the displacement information of both tissue layers obtained from the MR-images, a force-displacement relation for the skin/fat and the muscle layer can be postulated.

Due to the indenter head geometry, a deformation was achieved which could be clearly reconstructed and evaluated from the MR-images. The actual thickness of the skin/fat layer ($\mathrm{l}_{i,F}$) and the muscle layer ($\mathrm{l}_{i,M}$) at each deformation step was measured along the indentation axis, Fig. 4. With respect to the undeformed initial lengths of each layer (skin/fat: $\mathrm{l}_{0,F} = 32$ mm, muscle: $\mathrm{l}_{0,M} = 58$ mm), the actual displacement of the skin/ fat layer and the muscle layer could be derived. Assigning the measured indenter forces to the corresponding displacements, the force-displacement curves depicted in Fig. 5 for gluteal skin/fat and muscle tissue were obtained.

3. 3D-reconstruction, mesh generation and modelling

3.1. 3D-reconstruction

To perform a material optimization for gluteal skin/fat and muscle tissue, an FE model of the initially undeformed tissue configuration as well as the pelvic bone was built. Since the finite element mesh

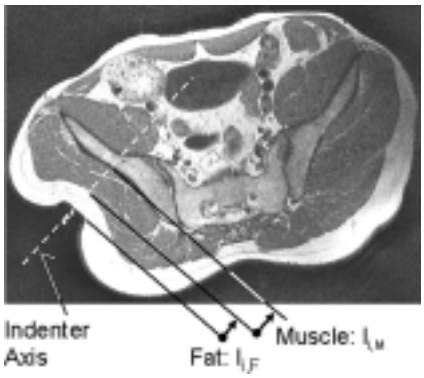

Fig. 4. Determination of the actual thicknesses of the deformed skin/fat and muscle layers.

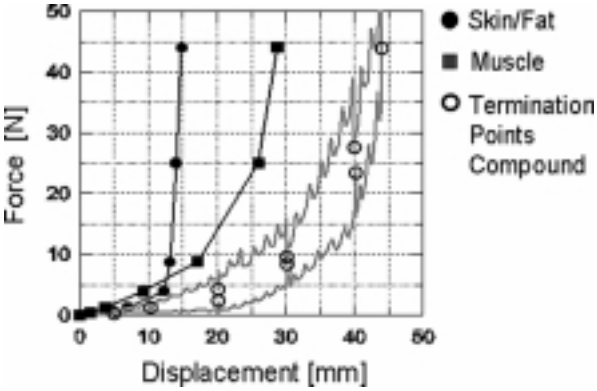

Fig. 5. Force-displacement data of human skin-fat-muscle compound tissue with termination points and separated elastic skin/fat and muscle force- displacement curves.

relies on surface data, these were derived from the MR images for the relevant buttock region, i.e. the right buttock cheek, using the image processing tool MIMICS® (Materialise, Leuven/Belgium). The reconstructed surfaces included the initial undeformed state of fat and muscle and bone as well as the deformed fat-muscle-boundary surface of all deformation steps and the position of the indentation axis.

3.2. Mesh generation

3.2.1. Compound Model

The reconstructed surface data was meshed using the HYPERMESH® (Altair, Michigan/USA) pre-processor. Both tissue components, skin/fat and muscle, were modelled with second-order tetrahedral continuum elements. The nodes in the fat-muscle-interface as well the muscle-bone-interface were rigidly connected. Thus, relative motion between the components was not assumed since shear stress was intended to be minimized by orienting the indentation axis accordingly, as described under 2.1.2. The bone structure as well as the indenter head were modelled as rigid bodies with the bone structure fixed in space and the indenter fully constrained, except in the indentation direction.

3.2.2. Skin/fat model and muscle model

To optimize the material parameters for skin/fat and muscle, the compound model was split into one model containing the skin/fat layer and another model containing the muscle layer with pelvic bone. To

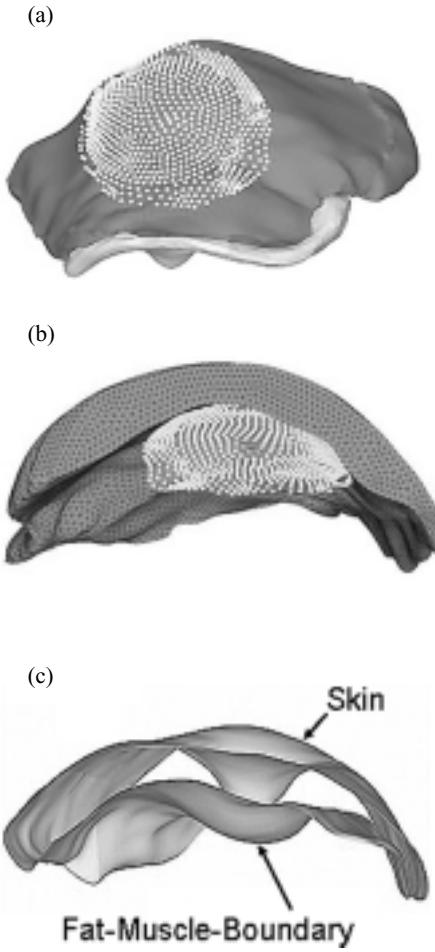

Fig. 6. (a) Muscle model (top side view) and (b) Skin/fat model (bottom side view) with prescribed nodes (highlighted), (c) Reconstructed deformed surfaces from MRI images with upper layer (skin) and deformed fat-muscle-boundary layer at an indentation displacement of 44 mm.

simulate both models separately, adequate boundary conditions were applied to both models. This was implemented by prescribing the nodes of the fat-muscle-boundary (Fig. 6c), i.e. the top surface nodes in the muscle-model (Fig. 6a) and the bottom surface nodes of the fat-model (Fig. 6b), such that they met all reconstructed fat-muscle-boundary layers of all deformation steps. The indenter head in the skin/fat model was moved accordingly. The assumption made hereby, is that the node prescriptions between the single deformed layers are normal to the particular deformed surface. Boundary conditions for the fat-muscle-boundary, i.e. the node displacements of the fat-muscle-boundary nodes were derived for the global directions via a coded routine.

4. Constitutive equation

The *in vivo* indentation testing of the skin/fat-muscle compound showed a viscoelastic material behaviour. In order to describe such phenomena, generally, a viscoelastic constitutive equation is adopted.

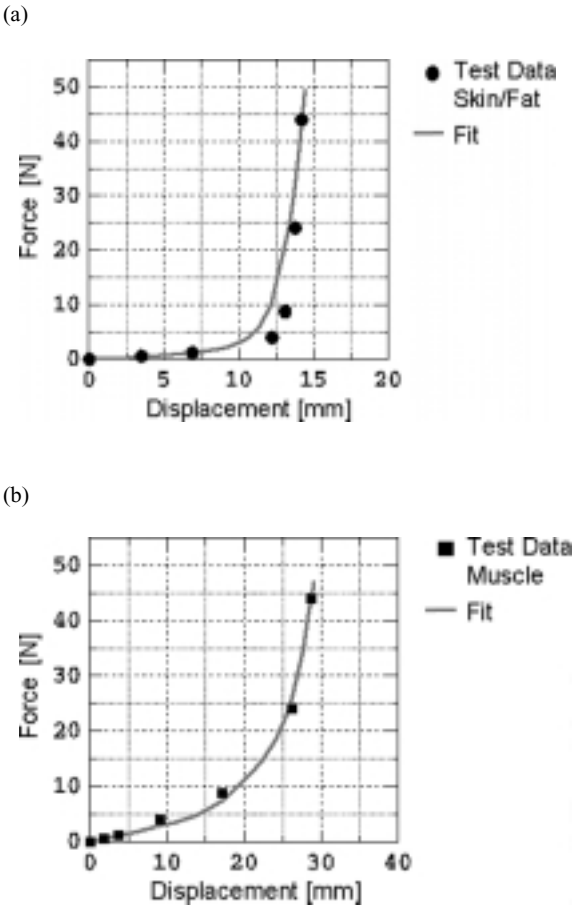

Fig. 7. Fit of the experimental data of the human gluteal (a) skin/fat tissue, (b) muscle tissue.

Viscoelastic models, in general, decompose the total stress tensor **S** into an (elastic) equilibrium stress part $\mathbf{S}_G$ and an overstress part $\mathbf{S}_{ov}$ representing the memory property of the material. Thus, the stress tensor can be written as $\mathbf{S} = \mathbf{S}_G + \mathbf{S}_{ov}$ as described in [8]. As previously mentioned, this study exclusively deals with the elastic properties of human tissue. Therefore, constitutive equations for hyperelasticity are permissible. For simplification, the index G in the above formula will be left out for further discussion.

The constitutive equation for nonlinear, hyperelastic, isotropic material behaviour in form of the CAUCHY stress tensor in spectral form reads [18]

$$\boldsymbol{S} = J^{-1} \sum_{i=1}^{3} \lambda_i \frac{\partial w}{\partial \lambda_i} \boldsymbol{n}_i \boldsymbol{n}_i \quad \text{with} \quad J = \lambda_1 \lambda_2 \lambda_3 \tag{1}$$

with the eigenvectors $\mathbf{n}_i$ of the left stretch tensor **V**, the principal stretches λ_i and the decomposed strain energy function w. For slightly compressible materials w reads

$$w = \sum_{k=1}^{N} 2 \frac{\mu_k}{\alpha_k^2} (\overline{\lambda}_1^{\alpha_k} + \overline{\lambda}_2^{\alpha_k} + \overline{\lambda}_3^{\alpha_k} - 3) + \sum_{k=1}^{N} \frac{1}{D_k} (J-1)^{2k} \tag{2}$$

where α_k, μ_k and D_k are material coefficients and $\overline{\lambda}_i := J^{-1/3}\lambda_i$ ($i = 1, 2, 3$) are the modified principle stretches. The initial shear and bulk modulus μ_0 and K_0 are given by [1]

$$\boldsymbol{\mu}_0 =: \sum_{i=1}^{N} \boldsymbol{\mu}_i \text{ and } K_0 = 2D_1^{-1} \tag{3}$$

Additionally, the following relations between the Poisson's ratio ν and the initial shear and bulk modulus and D_1 hold

$$v = \frac{3K_0/\mu_0 - 2}{6K_0/\mu_0 + 2} \text{ and } D_1 = \frac{3}{\mu_0}\frac{1-2v}{1+v} \tag{4}$$

With regard to Eqs (1) and (2) the following final constitutive equation for slightly compressible hyperelastic materials in terms of the principal stretches λ is obtained (for J see Eq. (1)):

$$\boldsymbol{S} = 2J^{-1}\sum_{i=1}^{3}\sum_{k=1}^{N}\left[\frac{\mu_k}{\alpha_k}J^{-\alpha_k/3}\left(\lambda_i^{\alpha_k} - \frac{1}{3}\sum_{j=1}^{3}\lambda_j^{\alpha_k}\right) + \frac{k}{D_k}J(J-1)^{2k-1}\right]\boldsymbol{n}_i\boldsymbol{n}_i \tag{5}$$

In this study, slight compressible material behaviour was assumed for human tissue according to Veronda and Westmann [33] and Fung [5]. Basically, constitutive equations of other forms than the OGDEN law may be used as long as they are capable of describing high deformations and distortions. These occurred in the testing procedure applied in this approach.

5. Parameter optimization

The basic idea in identifying appropriate material parameters for skin/fat and muscle which account for the test conditions is to simulate both models independently, parameterizing the material coefficients α_k, μ_k and D_2. The Poisson's ratio which was assumed to be $\nu = 0.495$ for both models accounting for slight compressibility was held constant during parameter optimization. Consequently, D_1 was determined from μ_0 and ν using Eq. 4b).

The optimization algorithm coded in Fortran and based on the deterministic SIMPLEX strategy [17] was coupled with the ABAQUS® (ABAQUS Inc., Rhode Island/USA) FE-solver following the inverse FE-method with the aim of finding a parameter setting which minimizes the objective function (6) subject to the following constraints: at each indenter deformation increment a) the prescribed nodes of the skin/fat and the muscle model are to meet the deformed fat-muscle-boundary surface reconstructed from the MR-images and b) simultaneously, the indenter force along the indentation axis in the skin/fat model as well as the reaction force along the indentation axis in the muscle model, both, obtained from property separation (Fig. 5), are to meet the measured force values obtained from the indentation experiment.

In this approach, the objective function Φ is defined by

$$\Phi := \sqrt[m]{\sum_{i=1}^{n}[f(h_i;\boldsymbol{p}) - f_i]^m} \stackrel{!}{=} \min \tag{6}$$

and is to minimize the deviation of the model function, i.e. the indenter force-displacement relation obtained from the simulation, from the target function, i.e. the indenter force-displacement relation

Table 1
In vivo material parameters for human gluteal skin/fat and muscle tissue

	[-]	[MPa]	[MPa^{-1}]
Skin/Fat	$\alpha_{1S/F} = -0.107647E+00$	$\mu_{1S/F} = 0.118261E-02$	$D_{1S/F} = 0.169117E+02$
	$\alpha_{2S/F} = -0.318953E+02$	$\mu_{2S/F} = 0.643855E-07$	$D_{2S/F} = 0.476897E+01$
Muscle	$\alpha_{1M} = 0.1316402E+01$	$\mu_{1M} = 0.102571E-02$	$D_{1M} = 0.194987E+02$
	$\alpha_{2M} = -0.1835933E+02$	$\mu_{2M} = 0.145209E-06$	$D_{2M} = 0.166315E+03$

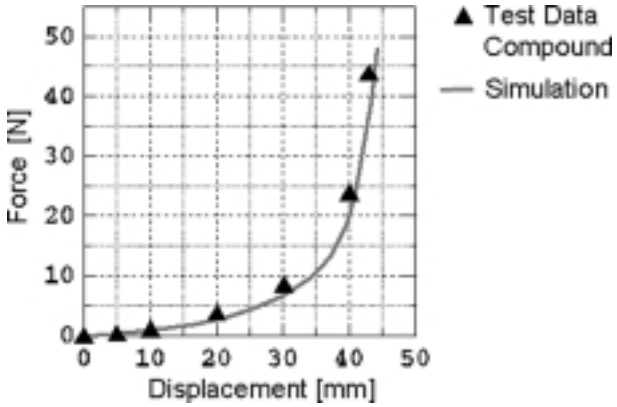

Fig. 8. Comparison of the simulation result with the experimental data.

obtained from the indentation experiment. In Eq. (6) n is the number of data points ($m, n \in R^+$), $f(h, \mathbf{p})$ is the model function, f_i are the measured data, h_i is the independent variable and $\mathbf{p}$ is the parameter vector of the model. It was found that an order of $N = 2$ of the series expansion in (2) fitted the experimental data with sufficient accuracy.

The results of the parameter optimization for the skin/fat model (Fig. 7a) and the muscle model (Fig. 7b) in comparison with the evaluated force-displacement curves show correlation factors of $R^2 = 0.957$ (skin/fat) and $R^2 = 0.998$ (muscle). The steep ascent of the experimental skin/fat data at high compressions could not be captured precisely, running 148 optimization iterations. The depicted muscle data fit was achieved after 93 iterations.

In Table 1 parameter values for human gluteal skin/fat tissue and for human gluteal muscle tissues are given.

The parameter values for skin/fat and muscle tissue exhibited stable material behaviour within the maximum nominal strain range reached when simulating the maximum indenter displacement.

6. Results

To verify the proposed approach, the optimized material parameters were assigned to the skin/fat and muscle parts of the compound model and the test conditions were simulated. A correlation factor of $R^2 = 0.997$ was found comparing the experimental data with the simulation result, Fig. 8.

A visual comparison of the deformed tissue shape of the simulation plot at maximum indenter displacement (Fig. 9a) with the corresponding MR slice image (Fig. 9b) is depicted in Fig. 9c as a superposition of the simulation result with the MR image.

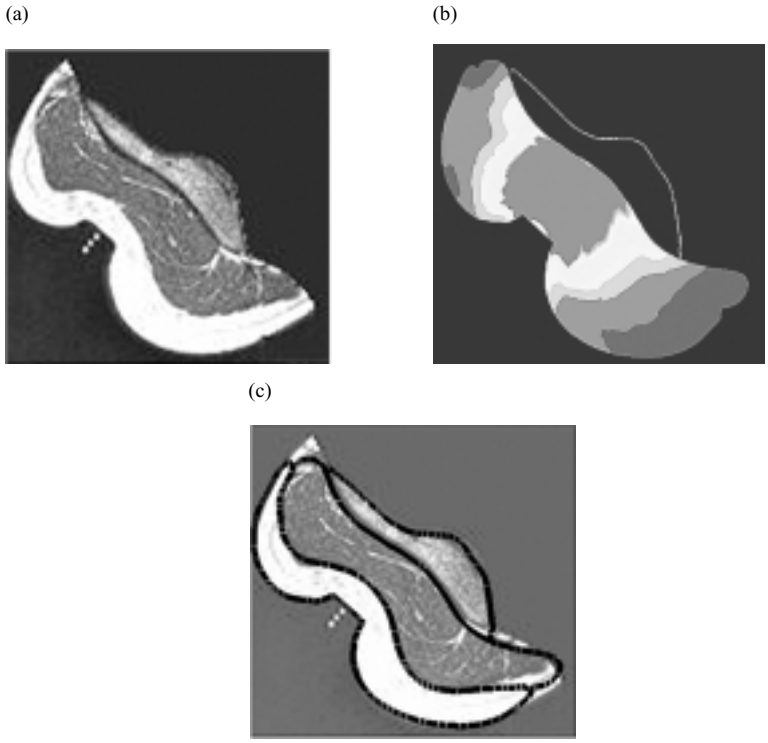

Fig. 9. Comparison of the MR image at 44 mm indenter displacement with the simulation result: (a) MR image, (b) Simulation (v. M. stress), (c) Superposition of MR image with simulation (borderline).

7. Discussion

An approach has been presented whereby the material parameters can be derived for human gluteal skin/fat and muscle, *in vivo*, using a combined technique of MR-imaging and computational simulation.

The material parameters for human gluteal skin/fat and muscle have been derived independently and then used for simulating the compound model. Reasonable accordance could be shown with the test data for the value-based comparison of the force-displacement results and the visually-based comparison of the deformed tissue structure. The approach was thus validated.

Since the force constraints used for parameter optimization were based on the long-term elastic material responses of skin/fat and muscle, the optimized parameters represent fully relaxed long-term elastic material behaviour. Therefore, the long-term shear moduli for human gluteal skin/fat and muscle tissue can be calculated from the optimized parameters, using Eq. (3a) for skin/fat: $G_{\infty,S/F} = \mu_{1,S/F} + \mu_{2,S/F} = 1182$ Pa and for muscle: $G_{\infty,M} = \mu_{1,M} + \mu_{2,M} = 1025$ Pa.

Compared to the derived long-term value for human gluteal muscle tissue, Gefen et al. [6] has reported that values for G_∞ for transversally loaded rat muscle tissue lay in the range of 345–730 Pa. These authors deduced that long-term transverse shear moduli of human skeletal muscles should be in the order of 250–1200 Pa. This deduction relied on *ex vivo* tensile tests of fresh human muscle fibers extracted during surgical treatment and *in vivo* elastography of human muscle. Both tests provided short-term shear moduli which are, according to Bosboom et al. [4] who employed rat tibialis anterior muscles, 1.6–2.0 times the long-term shear moduli. Palevski et al. [22] found long-term shear modulus values in the range of 700 ± 300 Pa, by performing transversal *ex vivo* indentation testing on porcine gluteus

muscles. Similarly to Bosboom et al., Palevski et al. have stated that for porcine gluteus muscle the instantaneous shear modulus is 7–14 times its long-term counterpart.

Derived material parameters for fully relaxed human gluteal muscle compare well with long-term shear modulus data of gluteal porcine muscle and estimations for human skeletal muscle. Comparable values for long-term shear moduli representing *in vivo* human gluteal skin and fat could not be found in the literature.

Furthermore, the corresponding long-term elastic moduli for human gluteal skin/fat and muscle soft tissue, assuming isotropic material behaviour, can be derived using the calculated long-term shear moduli as well as the relation $\mathrm{E}_\infty = 2(1+\upsilon)G_\infty$ for gluteal skin/fat to $\mathrm{E}_{\infty,S/F} = 3.53$ kPa and $\mathrm{E}_{\infty,M} = 3.1$ kPa for gluteal muscle tissue. These values are in accordance with the instantaneous values initially listed and used for FE simulations when downsizing the literature values with the proposed multipliers. Since tissue stress relaxes within seconds but pressure sores develop over minutes to hours, the exclusive use of instantaneous material constants will inaccurately reproduce the stress-strain distribution inside the tissue.

The mechanical tissue characterization described here leads to parameter sets for human gluteal skin/fat and muscle. These parameters, however, rely on measurements from one healthy male subject and therefore may not generally represent human gluteal soft tissue, since there may be substantial individual variability in the mechanical properties of soft tissue. To provide a parameter classification accounting e.g. for gender, age and state of health, a diverse subject study could reveal more detailed information.

The main objective of this investigation was to present a possible technique to establish biomechanical parameters for skin/fat and muscle tissue in the human gluteal region. Focus was laid upon the separation of the specific tissue components of the skin-fat-muscle compound and furthermore, the identification of the biomechanical parameters of the single tissue types. Although the derived parameters apply to only one individual, they correspond with the order of magnitude of human gluteal tissue long-term moduli as proposed in the literature stated above.

Presently, tissue characterization is being performed on a number of subjects to ratify the derived material parameter sets for human gluteal skin/fat and muscle and to provide a statistical foundation.

Acknowledgements

Preparatory work for this investigation was made in the course of the project ”Mechanische Charakterisierung humaner Weichgewebe (MeChum)” funded by the “Bundesministerium für Forschung und Technologie” of the Federal Republic of Germany.

References

[1] ABAQUS, User’s Manual, Version 6.1, Hibbitt, Karlsson and Sorensen, 2002.
[2] T. Aoki, T. Ohashi, T. Matsumoto and M. Sato, The pipette aspiration applied to the local stiffness measurement of soft tissues, *Ann Biomed Eng* **23** (1997).
[3] G. Bennett, C. Dealey and J. Posnett, The cost of pressure ulcers in the UK, *Age and Ageing* (2004).
[4] E.M. Bosboom, M.K. Hesselink, C.W. Oomens, C.V. Bouten, M.R. Drost and F.P. Baaijens, Passive Transverse Mechanical Properties of Skeletal Muscle Under In Vivo Compression, *J Biomech* (2001).
[5] Y.C. Fung, *Biomechanics: Mechanical Properties of Living Tissues*, Springer-Verlag, New York, 1993.
[6] A. Gefen, N. Gefen, E. Linder-Ganz and S.S. Margulies, In Vivo Muscle Stiffening Under Bone Compression Promotes Deep Pressure Sores, *ASME J Biomech Eng* (2005).

[7] A. Gefen, M. Megido-Ravid, M. Azariah, Y. Itzchak and M. Arcan, Integration of plantar soft tissue stiffness measurements in routine MRI of the diabetic foot, *Clinical Biomechanics* (2001).
[8] S. Hartmann, Numerical studies on the identification of the material parameters of Rivlin's hyperelasticity using tension-torsion tests, *Acta Mechanica* (2001).
[9] S. Hartmann, T. Tschöpe, L. Schreiber and P. Haupt, Large Deformations of a Carbon Black-Filled Rubber. Experiment, Optical Measurement and Parameter Identification Using Finite Elements, *European Journal of Mechanics – Series A/Solids* **22** (2003), 309–324.
[10] A.G. James, A. Green and G.M. Simpson, Strain energy functions of rubber. I. Characterization of gum vulcanizates, *Applied Polymeric Science* (1974), 2033–2058.
[11] S.L. Knight, R.P. Taylor, A.A. Polliack and D.L. Bader, Establishing predictive indicators for the status of loaded soft tissues, *Journal of Applied Physiology* (2001).
[12] M. Kosiak, Etiology and Pathology of Ischemic Ulcers, *Arch Phys Med Rehabil* (1959).
[13] D. Lim, F. Lin, R. Hendri and M. Makhsous, Finite Element Analysis for Evaluation of Internal Mechanical Responses in Buttock Structure in a True Sitting Posture: Development and Validation, *RESNA 29th Int Conf* (2006).
[14] E. Linder-Ganz and A. Gefen, Assessment of mechanical conditions in sub-dermal tissues during sitting: A combined experimental-MRI and finite element approach, *Journal of Biomechanic* (2007).
[15] E. Linder-Ganz and A. Gefen, Risk factors for deep pressure sores reveald through finite element simulations coupled with an injury threshold and a damage law for muscle tissue, *Proceedings of BIO2006* (2006).
[16] A. Lion, Constitutive Model for Carbon Black Filler Rubber: Experimental Results and Mathematical Representation, *Continuum, Mechanics & Thermodynamics* **8** (1996), 153–169.
[17] J.A. Nelder and R. Mead, A simple Method for function minimisation, *Comp J* **7** (1969).
[18] R.W. Ogden, Large Deformation Isotropic Elasticity: On the Correlation of Theory and Experiment for Compressible Rubberlike Solids, *Proceedings of the Royal Society of London* (1972).
[19] C.W.J. Oomens, O.F.J.T. Bressers, E.M.H. Bosboom, C.V.C. Bouten and D.L. Bader, Can Loaded Interface Characteristics Influence Strain Distributions in Muscle Adjacent to Bony Prominences? *Computer Methods in Biomechanics and Biomedical Engineering* **6**(3) (2003).
[20] C.W.J. Oomens, O.F.J.T. Bressers, E.M.H. Bosboom and C.V.C. Bouten, Deformation Analysis of a Supported Buttock Contact, *Bioengineering Conference BED-Vol. 50, ASME* (2001).
[21] C.W.J. Oomens, M.R. Van Ratingen, J.D. Janssen, J.J. Kok and M.A.N. Hendricks, A numerical–experimental method for a mechanical characterisation of biological materials, *Journal of Biomechanics* (1993).
[22] A. Palevski, I. Glaich, S. Portnoy, E. Linder-Ganz and A. Gefen, Stress relaxation of porcine gluteus muscle subjected to sudden transverse deformation as related to pressure sore modeling, *Journal of Biomechanical Engineering* (2006).
[23] P.R. Quintavalle, C.H. Lyder, P.J. Mertz, C. Phillips-Jones and M. Dyson, Use of High-Resolution, High-Frequency Diagnostic Ultrasound to Investigate the Pathogenesis of Pressure Ulcer Development, *Skin & Wound Care* (2006).
[24] E.M. Romanus, Microculatory reactions to controlled tissue ischaemia and temperature: a vital microscopic study on the hamster's cheek pouch, *Journal of Tissue Viability* (2006).
[25] M. Schrodt, G. Benderoth, A. Kühhorn and G. Silber, Hyperelastic description of polymer soft foams at finite deformations, *Technische Mechanik* **25**(3–4) (2005), 162–173.
[26] M. Schrodt, Experimentelle und numerische Untersuchungen zur Dekubitusproblematik am Beispiel des Fersen-Schaumstoff-Kontaktbereiches, Dissertation, Berlin, 2006.
[27] M.B. Silver-Thorn, E. Tonuk and J. Kemp, In Vivo Indentation of Lower Extremity Limb Soft Tissues, *IEEE Trans Rehabil Eng* (1999).
[28] A. Stekelenburg, C.W.J. Oomens, C.J. Strijkers, L. de Graaf, D.L. Bader and K. Nicolay, A new MR-compatible loading device to study in vivo muscle damage development in rats due to compressive loading, *Medical Engineering and Physics* (2005).
[29] Q. Sun, F. Lin, S. Al-Saeede, L. Ruberte, E. Nam, R. Hendrix and M. Makhsous, Finite element modeling of human buttock-thigh tissue in a seated posture, Bioengineering Conference, Colorado (2005).
[30] Q. Sun, F. Lin, S. Al-Saeede, L. Ruberte, E. Nam, R. Hendrix and M. Makhsous, Soft Tissue Stress in Buttock-Thigh of a Seated Individual Elucidated by a 3D FE Model, *RESNA 28th Int Conf* (2005).
[31] M. Tada, N. Nagai and T. Maeno, Material Properties Estimation of Layered Soft Tissue Based on MR observation and Iterative FE Simulation, MICCAI, 8th International Conference, 2005.
[32] B.A. Todd and G.J. Thacker, Three-dimensional computer model of the human buttocks *in vivo*, *Journal of Rehabilitation Research and Development* **31**(2) (1994).
[33] D.R. Veronda and R.A. Westmann, Mechanical Characterization of Skin-Finite Deformations, *Journal of Biomechanics* **3** (1970).
[34] V. Vuskovic, M. Kauer, J. Dual and M. Bajka, Method and device for in-vivo measurement of elasto-mechanical properties of soft biological tissues, *Machine Graphics & Vision International Journal* **8**(4) (1999).